CHALMERS
UNIVERSITY OF TECHNOLOGY

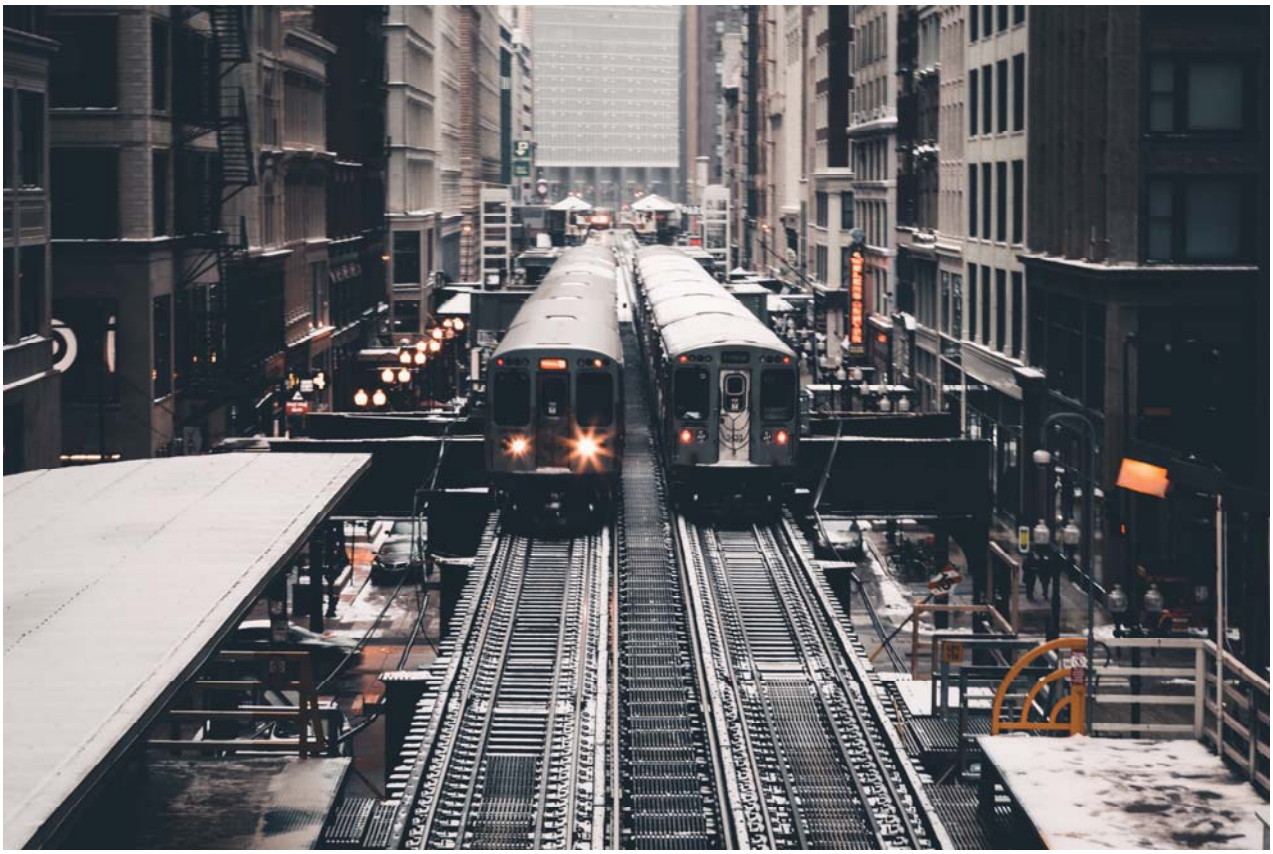

Train vibrations and site effect estimation

Using ambient vibration measurement to estimate amplification of vibrations from trains

Master's thesis in Applied Acoustics

GUSTAF FRID

Department of Architecture and Civil Engineering
Division of Applied Acoustics
Vibroacoustics Group
CHALMERS UNIVERSITY OF TECHNOLOGY
Master's Thesis BOMX02-18-08
Gothenburg, Sweden 2019

MASTER'S THESIS BOMX02-18-08

Train vibrations and site effect estimation

Using ambient vibration measurement to estimate amplification of vibrations from trains

Master's Thesis in the Master's Programme Sound and Vibration

GUSTAF FRID

Department of Architecture and Civil Engineering
Division of Applied Acoustics
Vibroacoustics Group
CHALMERS UNIVERSITY OF TECHNOLOGY
Göteborg, Sweden 2019

Train vibrations and site effect estimation

Using ambient vibration measurement to estimate amplification of vibrations from trains

Master's Thesis in the Master's Programme Master's Sound and Vibration

GUSTAF FRID

Examensarbete BOMX02-18-08
Institutionen för arkitektur och samhällsbyggnadsteknik
Chalmers tekniska högskola, 2019

Department of Architecture and Civil Engineering
Division of Applied Acoustics
Vibroacoustics Group
Chalmers University of Technology
SE-412 96 Göteborg
Sweden
Telephone: + 46 (0)31-772 1000

Cover:
The picture downloaded from Pexels.com and is free to use for commercial and non-commercial purposes. It has nothing to do with the thesis except that a train is featured.

Department of Architecture and Civil Engineering
Göteborg, Sweden, 2019

Train vibrations and site effect estimation
Using ambient vibration measurement to predict amplification of vibrations
Master's Thesis in the Master's programme in Sound and Vibration
GUSTAF FRID
Department of Civil and Environmental Engineering
Division of Applied Acoustics
Vibroacoustics Group
Chalmers University of Technology

Abstract

Train induced vibrations are known to cause annoyance and sleeping disorders among people living close to rail roads. This and other problems arising around train vibrations are brought up to date as the current government as well as previous ones suggest building of high speed train routes. The methods, commonly used in Sweden, for predicting levels of train induced vibrations are semi-empirical meaning that a formula is used in which site specific constants require measurements at the site to determine their value.

This thesis aims to study amplification of vibrations whose source are train passages. Specifically the fundamental frequency, having a wavelength corresponding to four times the soil depth is subject for the analysis. A method frequently used by seismologists to estimate amplification of earth quakes at certain sites is used. By measuring ambient vibrations with a three-axial accelerometer or geophone and dividing the mean of the two spectra of the horisontal components by that of the vertical, the fundamental frequency, f_0, will be indicated by a peak in the resulting spectrum, called the H/V-ratio. The method can also, to some extent, estimate the amplification factor at f_0.

The effect of f_0 on train vibration is studied in three steps. In the first step, measurement results from previous studies are studied with regard to f_0, derived from soil depth maps and estimated deformation parameters. For the next step, FEM calculations are carried out studying transfer functions at the surface of a soil deposit with soil depth as parameter. Material parameters are chosen so that the fundamental frequency should appear within the studied frequency range. Also, measurements are performed using the H/V-ratio technique. At a meadow adjacent to a rail road, ambient vibra-

tions are measured as well as vibrations from trains passing by close to and further away from the rail in order to obtain a transfer function. The spectra obtained from the train passages at each point, as well as the transfer functions, are compared with the corresponding H/V-ratio to see if there is amplification at f_0.

The results from the literature study indicate that f_0 does play a role in that sense that wave propagation below that frequency cannot occur, theoretically. The study of previously made measurements confirms this as sites with a high estimated f_0 are not subject to high vibration levels. The FEM calculations also show a dependency of transmitted wave energy on soil depth in that sense that there is a frequency below which there is very weak wave propagation. The response spectra at 10 m and 40 m as well as the transfer function from the source to the field point also inherit a peak at this frequency which is one third octave lower than the expected fundamental frequency, concerning the vertical component.

As for the measurements, no conclusions can be made as the measurement equipment used was not sensitive enough to capture ambience. Nevertheless, the peaks in the H/V-ratio, although weak, appear at the same frequencies as those at which amplification occur in the measurement of train passages. It cannot be concluded, but also not excluded, that the difference in the measured spectra at the different points depend on f_0.

Keywords: Train induced vibrations, site effect estimation, ambient vibra- tion, geodynamics

Contents

Acknowledgements

I would like to express my deepest gratitude to all those who have helped me finishing this thesis. Not everyone will be payed attention to here but before I let this masterpiece be forever shelved I would like to mention at least a few. First of all I wish to thank my supervisor Patrik Höstmad who have been patient enough to deal with me and my report, although sporadically, for a much too long time. The staff at Technical Acoustics at Chalmers also deserve great appreciation - especially Börje and Lars. My colleges at work - first at Tyréns then at Brekke & Strand - have also been indispensable, not the least for lending me measurement equipment but also for good advice, encouragement and sometimes slightly mean but well meant insinuations that this work has been taken much too long. Finally, since they probably are the only ones who will read this, I cannot help but sending some love to my family - Kristina who happened to become my wife by the time this thesis should have been done and our two boys who came afterwards. I could blame you for being the biggest reason to procrastinate but at the same time you have been the inspiration which finally made me finish.

1. Introduction

1.1. Background

A number of suggestions on how to expand the Swedish railway system have been discussed and investigated by Swedish authorities. High speed trains are mentioned in, for example, [1], [15] and [6]. Some of the ambitions mentioned in the most recent investigation, Sverigeförhandlingen [22], is to reduce environmental impact of transport, reduce travel time between large cities, increase capacity and making the Swedish railway compatible with European railways. The strength of railways connecting urban areas is also a weakness as trains, apart from making noise, induce vibrations that propagate in the ground and into buildings near the track. Research concludes that vibration in buildings causes annoyance and sleeping disorder which in the long term can have negative effects on the health for people living in houses near a frequently trafficated track [18] , [25].

In order to predict the impact of vibration, the methods commonly used are based on correction factors representing source, propagation path and receiver [28]. These factors are multiplied to the source amplitude in order to predict a vibration level at the receiver. Determination of these correction factors are mostly site specific and based on statistical data from numerous measurements [7], [14].

In seismology, site effect estimation is necessary when designing buildings in areas with large seismic hazard [26]. Site effect estimation consists of determining freqencies at which amplification occurs and the degree of amplification. Among several methods of determining the site effects at a certain location, the H/V-ratio is a cheap and easy method which is based on ambient vibration measurement. By measuring ambient vibrations triaxially, a fundamental frequency at which amplification occurs, will be predominating in the resulting spectrum when dividing the mean of the horisontal response spectra with the vertical [24].

1.2. Purpose and goal

The purpose of this thesis is to investigate if seismological site effect estimation has a potential to be applied on prediction of train induced vibration levels. By measurements and simulations it is investigated if an eventual amplification factor from a point close to the rail to point further away depend on the fundamental frequency of the soil deposit.

1.3. Limitations

As the H/V-ratio primarily gives the fundamental frequency of a soil deposit, only this frequency will be considered in the analysis and it will be determined by observing plots over frequency responses whereas the amplification factor is not considered.

In the finite element calculations, a linear elastic material will be used although soil dynamics in general are associated with non-linear behaviour. Also, only soil depth will be the only parameter studied in the finite element method. Layering of soils with different wave speed that leads to refraction effects will not be considered.

1.4. Outline of the thesis

This thesis constists of 7 chapters whose content are shortly summarized in this section. The current chapter, the first, serves for the reader as an introduction to the subject with a short background leading to the purpose of the study. The second chapter summarizes existing methods for predicting train vibrations. In the third chapter the theory of soil dynamics in general is briefly described as well as the more specific theory of train induced vibrations, human response to vibrations and resonances in soil deposits. Also accounted for is the theory behind the measurement method and the calculation method used in the study. The forth chapter describes each step in which the study is performed and the fifth chapter serves as a reflection of the forth giving the results of each step. Finally the last chapters, chapter 6 and 7, are devoted to discussion and conclusion respectively.

2. Semi-empirical models for predicting train induced vibrations in Scandinavia

The most common methods used for predicting vibration levels due to train traffic are semi-empirical. That means a theoretical formula is used with which the vibration level on the ground or in a building at a certain site can be calculated by inserting parameters that are specific for this site. The formula is generally expressed as a Green's function for semi-infinite spaces. Thus, the minimum input required for the calculation is source strength, a damping factor for the propagation path and a distance to the receiver. If the vibration level in a building is to be considered another factor could be introduced in addition to the Green's function. In this chapter, a couple of studies made on different sites in order to obtain a prediction formula are presented.

2.1. TVANE

As a part of the project TVANE which studied human perception of noise and vibration from rail and road bound traffic, vibration measurements were carried out at four different sites in south western Sweden [17]. At two of the sites, Töreboda and Falköping, vibration levels were known to be low, why only a few measurements were carried out in order to confirm this information. At the other two sites, Kungsbacka and Alingsås, the vibration levels were known to be high why more thorough measurements were carried out. For these sites, a calculation model suggested by [3] and shown in (2.1) for vertical vibrations is adapted according to the measurement results from the different sites.

$$v = mr^k \tag{2.1}$$

where m is the source strength, r is the distance to the receiver and k a constant describing the geological conditions. The measurements were performed using two geophones on the ground measuring vertical velocity in order to obtain the attenuation constant. Two triaxial vibrometer was placed inside the house measuring vibration in vertical as well as horisontal direction. For the sites in both Alingsås and Kungsbacka it was possible to obtain constants used to predict vibrations on the ground, but only for the site Kungsbacka the formula could be adapted to calculate vibration levels in buildings at the site. In Alingsås, the vibrations were sometimes five times larger than on

the ground. The authors of [17] refers to the sensitivities of the buildings as the most probable reason to why the model fails for the site in Alingsås, as the model does not take resonances in buildings into account. To obtain such information, more thorough investigation on the structures of the buildings is necessary, according to [17]. It could be concluded, however, that the highest level was detected on the second floor, in the horisontal component and with a frequency at around 5 Hz for both of the sites.

2.2. ENVIB

A large study with the aim to create a semi-empirical model that could be implemented in GIS was made by [14]. Measurements of train passages were carried out at several sites in Sweden in order to obtain a function for wave propagation expressed as

$$v = v_0 \left(\frac{r}{r_0} \right)^{-n} e^{-\alpha(r-r_0)} \tag{2.2}$$

where v_0 is the particle velocity at the reference point, r is the distance to the source r_0, the distance to the reference point from the actual source, n is the power of geometric attenuation and α is the damping. The train passages were recorded using geophones and accelerometers on the sleeper, on the ballast near the track as well as several spots at different distances from the track. With the measurement results, the site specific parameters in the formula was adjusted for each of the sites. The importance of geological conditions were studied in that sense that passages with similar properties such as train type, train speed and embankment height were studied leaving the geotechnical conditions as the main variable. The conclusion from that was that geotechnical conditions have an effect, but no conclusion about which the most important factors are is made. The author also mentions vibrations in buildings and that although the vertical component on the ground often has higher level than the horisontal, the opposite may occur inside buildings. However, no conclusion about the effect on buildings can be made as there is not enough measurement data to perform a statistical analysis.

2.3. Banedanmarks Nye Vibrationsmodel

On behalf of Bane Danmark, COWI developed a frequency dependent empirical model for predicting vibration levels in buildings. The vibration level at the receiving point is expressed as

$$L_{\alpha j} = L_{\alpha k} + TL_i \tag{2.3}$$

where $L_{\alpha k}$ is the source level and TL_i represents correction factors for various properties of the propagation path such as geology and interaction between soil and structure

for example. Each of the source and correction factors are expressed in third-octave band ranging from 1,25 Hz to 160 Hz. The data for the study consisted of around 2000 train passages in order to define source strength parameters of typical danish trains. In order to see the influence of geological conditions, train passages at 16 different sites were analysed. The vibration levels in 200 buildings were measured in order to see the response of typical buildings. The study concludes that there is a small or even neglible correlation between train speed and vibration level unlike other studies like for example [14]. For the geometrical damping a function similar to those in [14] and [17] is used to calculate the vibration level, a, at an arbitrary point on the ground, expressed in (2.4).

$$a = a_k \left(\frac{r_k}{r}\right)^{m(f)} \tag{2.4}$$

where a_k is the level at the reference point, r_k is the distance from the source to the reference point, r is the distance from the source to the reference point and $m(f)$ is a frequency dependent function representing damping and eventual amplification. The last factor in the expression describes the damping for which η is the viscous damping constant. Unlike other studies, [5] makes corrections for the fact that the ground, especially for low frequencies, cannot be regarded as a semi-infinite space which is the assumption made for the propagation functions (2.1) and (2.2). In addition, $m(f)$ takes into account the resonance frequency, f_0, for compression waves of the ground. This frequency is calculated from the soil depth, Poisson's ratio, and estimated wave speed for the soil type at the site.

$$m(f) = 1 - e^{\left(\frac{f}{f_b}\right)} + \frac{b\left(\frac{r_j}{r_k}\right)^a \left(\frac{f}{f_0}\right)}{\left(\frac{f_0 - f}{f_0}\right)^2 \left(\frac{f}{f_0}\right)^2} \tag{2.5}$$

where $a = 0,3$ according to measurements from one of the studied objects, $b = 1$ if the soil is considered layered, otherwise $b = 0$. $f_b = c/r_k$ and denotes the frequency at which the wave front shifts from plane to curved.

3. Soil dynamics, train vibrations and site effects

In this chapter, some basic concepts of soil dynamics and train vibrations are presented as well as the theory behind the Finite Element Method and H/V-method who are used in the analysis.

3.1. Elastic wave propagation

This section gives a review on the theory of elastic waves. In subsection 3.1.1, an infinite, homogenous, isotropic and elastic space is described for which the formulation and solution of the wave equation is relatively comprehensible. In the following subsection, 3.1.2, the semi infite elastic space is presented but without any further derivations.

3.1.1. Infinte elastic medium

The following derivation of the wave equation originates from Prakash, [19]. In an infinite elastic medium, two types of waves exist. These are the so called body waves, i.e. compression waves and shear waves. The formulation of the wave equation starts with a translational equilibrium for an infinitesimal element. Equation (3.1) shows the equilibrium equation along x-axis. Where similar expressions are used for the x-, y- and z-axis, only that for the x-axis is written. This applies to Equation (3.1), (3.4), (3.21), (3.6), (3.7) and (3.10).

$$\frac{\delta \sigma_x}{\delta x} + \frac{\delta \tau_{xy}}{\delta y} + \frac{\delta \tau zy}{\delta z} = \rho \frac{\delta^2 u}{\delta t^2} \tag{3.1}$$

Here, u denotes the displacement along the x-axis. Correspondingly, v and w are displacements along y- and z-axis relatively. The Lamé constants,

$$G = \frac{E}{2(1+\nu)} \tag{3.2}$$

$$\lambda = \frac{\nu E}{(1+\nu)(1-2\nu)} \tag{3.3}$$

where ν is the Poisson's ratio, are used to express the stresses in (3.1) in terms of displacements as such:

$$\sigma_x = \lambda \bar{\epsilon} \quad \tau_{xy} = \tau_{yx} = G\gamma_{xy} \tag{3.4}$$

where ϵ_x is normal strain along the x-axis, γ is shear strain and $\bar{\epsilon} = \epsilon_x + \epsilon_y + \epsilon_z$
Expressing strain and rotation in terms of displacements as

$$\epsilon_x = \frac{\delta \tau_{xy}}{\delta y} \quad \gamma_{xy} = \frac{\delta v}{\delta x} + \frac{\delta u}{\delta y} \qquad (3.5) \qquad 2\bar{\omega} = \frac{\delta w}{\delta y} + \frac{\delta v}{\delta z} \qquad (3.6)$$

leads to the following formulation of the wave equation:

$$\rho \frac{\delta^2 u}{\delta t^2} = (\lambda + G) \frac{\bar{\epsilon}_{xz}}{\delta z} + G \nabla^2 u \qquad (3.7)$$

where ∇^2 is the spatial differential operator:

$$\nabla^2 = \frac{\delta^2}{\delta x^2} + \frac{\delta^2}{\delta y^2} + \frac{\delta^2}{\delta z^2} \qquad (3.8)$$

In the infinite space, the wave equation has two solutions each representing the two types of body waves; the compression wave, (3.9), and the shear wave, (3.10).

$$\frac{\delta^2 \bar{\epsilon}}{\delta t^2} = v_c^2 \nabla^2 \bar{\epsilon} \qquad (3.9) \qquad \frac{\delta^2 \bar{\omega}}{\delta t^2} = v_s^2 \nabla^2 \bar{\omega} \qquad (3.10)$$

where v_c and v_s are the propagation velocities for compression and shear waves respectively.

$$v_c = \frac{E_b}{\rho} \qquad (3.11) \qquad v_s = \frac{G}{\rho} \qquad (3.12)$$

3.1.2. Semi-infinite elastic medium

By applying a boundary on the elastic medium, making it semi-infinite, the solution of the wave equation (3.7) requires definition of boundary conditions. The procedure of determining these is described by Lamb, [13], but will not be further explained in this thesis. An important result of the wave equation solution for semi-infinite medium, however, is the occurence of surface waves of which the Rayleigh wave is the most important. The Rayleigh wave appears near the boundary of the half-space having a retrograde elliptical motion. Considering an oscillating point source on the surface of semi-infinite medium, a wave field is made up, consisting of body waves, i.e. compression waves and shear waves as well as Rayleigh waves. The geometrical attenuation of body waves is mainly $1/r$ except from along the surface where it is $1/r^2$, with r being the distance from the point source. As for Rayleigh waves, the attenuation along the surface is $1/\sqrt{r}$. Furthermore, the input energy on the point source is divided such, that two thirds are transmitted as Rayleigh waves [19].

3.2. Physics of train vibraitons

This section covers briefly the theory on how vibrations from trains are generated, how they propagate in the ground and finally transmitted to a building. Statements are collected from theoretical research as well as findings from empirical and numerical studies.

3.2.1. Generation

An idealized model described by Krylov, [12], gives that train vibrations are generated by deflection of the rail track which in turn makes the sleepers, on which the track rests, move as dynamic vertical forces as a train passes by. Thus, vibrations are created even if track and wheels are ideally flat and the frequency content of a train passage is directly dependent on train speed and distance between the wheels and wheel axles through which the train load is transmitted. Kouroussis et. al [11] lists various additional excitation mechanisms and to which frequency ranges they are associated with. For example, in the low frequency range, below 15 Hz, the phenomenon with axle passages described above is present but also bouncing of the car body when defects on rail or wheel excites the natural frequencies of the car. Both [12] and [11] also mentions the dependence of the ratio of train speed and Rayleigh wave speed, also called the Mach number, on the vibration amplitude. Vibration amplitudes starts to increase rapidly when the Mach number exceeds $0,5$ [11].

3.2.2. Propagation

The theoretical basis for propagation of ground vibrations and especially of Rayleigh waves from a point source on the surface of a homogenous elastic half-space was provided by Lamb, [13] and is briefly explained in Section 3.1. Among the comments on discrepancies between theory and observation the author mentions the fact that propagation can be affected by heterogenities of the soil if these are in a scale compared to the wave length. Also, wave propagatation in loose soil over solid rock could be modified locally but with high irregularities. As for body waves, who would propagate radially from a point source, the theoretical geometrical attenuation relation ship is Ar^{-1} except at the surface of the half space where the attenuation is Ar^{-2} [19]. In a study by Auersch and Said [4] it was found that the attenuation of ground borne waves is considerably higher than the theoretically expected as material or scattering damping is the most important factor. The effect of soil depth, which is more often discussed in terms of earth quakes as explained in Section 3.5, is also discussed in terms of local sources. Massarch et al. [20] claims that wave propagation theoretically cannot occur below frequencies with a wavelength equal to four times the soil depth. What could be contradictory to this statement is that amplitudes increase with decreasing soil depth

as the wave energy is concentrated and excites less material [7]. The authors do not, however, mention if this statement is valid for a certain frequency range.

3.2.3. Reception

Srbulov, [21], describes two types of soil-structure interaction used to explain motions in buildings due to ground vibrations that can either be amplified or attenuated. If the foundation of a building exhibits a stiffness that is larger than that of the ground, the amplitudes of the ground vibrations will be averaged. This is called kinematic interaction. Inertial interaction is when ground vibrations are transmitted to a structure exciting movement in its masses which make the structure reradiate waves to the ground. This causes superposition of incoming and outgoing waves which could cause resonant behaviour if the resonance frequencies of the ground and the building are similar. For the coupling loss between ground and foundation, Hanson et al. [7] gives a rule of thumb saying that the heavier the foundation, the higher coupling loss.

3.3. Human response to train vibrations

Ground borne vibrations from trains can cause annoyance in terms of perceived vibration, rattle of items on shelves or ground borne vibrations reradiated as sound from vibration room surfaces, as stated by several researchers such as [25] and [7]. There have been attempts to find a correlation between vibration amplitude and annoyance by for example Klaeboe et al. [9]. They estimated vibration amplitude using a semi-empirical model and performed interviews with dwellers living in the vicinity of a railway. Without studying in what fashion vibrations where perceived (mentioned above), they found a correlation between estimated amplitude and annoyance. Furthermore, perceived vibration from trains can have an impact on the annoyance of noise from the same. Both Öhrström et al. [18] as well as Howarth and Griffin [8] found that highly perceived vibration together with train noise reduced the level at which the latter was perceived as annoying. On the other hand, other research has found that noise could have a masking effect on vibration as the threshold for vibration perception was higher when combined with a certain level of broad band noise [16] [10].

3.4. Local amplification of ground bourne vibrations

In seismology, it has been noticed that the amplitude of earthquakes is not only dependent on the distance from the epicentrum but that the geological conditions at a site can have considerable impact on the earthquake response. Due to reflections of ground borne waves at bedrock and at the surface a site with soft soil exhibits a fundamental

frequency as well as higher resonance frequencies at which the vibrations are amplified [**?**]. The fundamental frequency, f_0, is also mentioned in the context of train vibrations by [20]. According to this study, no wave energy can propagate below f_0. Vibrations with frequency corresponding to f_0 are amplified to varying extent depending on the impedance difference between the soil layers or the bedrock and the homogenity of the soil layer. The fundamental frequency of a soil layer, f_0, depends on the thickness, h, of the soil layer and the shear wave speed, V_S, of the soil.

$$f_0 = \frac{V_S}{4h} \tag{3.13}$$

A number of methods for estimating these site effects are available. In this thesis, methods using ambient vibration measurement are used. These are relatively easy performed and cost effective methods who in many cases provides with sufficiently accurate results. When measuring ground or building vibrations it is assumed that the wave field in the ground and on its surface, originated from sources such as traffic, weather and industry, together represent sources that are equally distributed in space and frequency. Therefore, in the case of ground vibrations - the fundamental frequency of the soil substructure or in the case of building vibrations - eigenfrequencies belonging to building modes should prevail when measuring ambient vibrations.

3.5. The H/V ratio

In 1989 [23] proposed a method for estimating transfer functions of soil substructures by analysing microtremor on the soil surface. By measuring ambient vibration in vertical and horizontal direction on the surface the shear wave fundamental frequency for the substructure can be detected by taking the ratio of the horizontal and vertical spectra from the measurement. What happens, according to [23], is that the effect of Rayleigh waves is eliminated from the horizontal spectrum, assuming that the effect is equal for vertical and horizontal components. Thus, the prevailing frequency of the H/V-spectrum is a result of multiple reflections of shear waves. The explanation in more detail originates from the general definition of the transfer function from the firm substrate to the soil surface: (In the following expressions, subscript H is for horizontal, V for vertical, S for surface and B for bottom.)

$$S_T = S_{HS}/S_{HB} \tag{3.14}$$

where S_{HS} is the horizontal spectrum of the surface and S_{HB} is the horizontal spectrum of the bottom of the substructure. Because S_{HS} contains the effect of surface waves,

$$E_S = S_{VS}/S_{VB} \tag{3.15}$$

representing the effect of Rayleigh waves on the vertical tremor, yields a more precise transfer function given as:

$$S_{TT} = S_T / E_S = R_S / R_B \tag{3.16}$$

where R is the H/V-ratio at the firm substrate and the soil surface respectively. It can be considered, according to [23], that $R_B = 1$ for a wide frequency range, as measurements have shown that the wave propagation on the firm substrate is even in all directions. Therefore, the transfer function could be estimated from the H/V-spectrum at the surface.

$$S_{TT} = R_B \tag{3.17}$$

3.5.1. Limitations of the H/V-ratio

Although [23] claims that the H/V-ratio can be regarded as a transfer function, other researchers point out that the main scope of performing an H/V-measurement should be to detect a fundamental frequency in the ground whereas it is not possible to accurately determine an amplification factor. Studies that compare more accurate but more costly methods for estimating site effect with the H/V-ratio method conclude that the latter method in general successfully estimates the prevailing frequency but not the amplification factor which is generally underestimated [2].

3.5.2. The SESAME project

The SESAME project (SESAME = Site EffectS assessment using AMbient Excitations) is a research project providing user guidelines on how to perform a site effect analysis with the H/V-ratio technique. The guidelines includes information on how to perform the actual measurement, requirements for performing a measurement, how to process the signaland how to interpret the results[2].

3.6. Finite Element methods and elastic waves

This section is an elemental summary of the finite element method from [34]. The finite element method is a numerical method used to approximate the physical state of a continuous entity by dividing it into a discrete number of subdomains, i.e. finite elements, interconnected by nodes. For each element, relations between the physical parameters can be expressed and for a structural dynamic problem these relations are often expressed in terms of nodal displacement. Having established relations between nodes for each single element, these are assembled in a global matrix equation in which all nodes are accounted for.

Figure 3.1.: Shape functions for a two dimensional element with four nodes.

3.6.1. Equations for a finite element

In the following, a two dimensional static loading problem is considered. Displacement and force are vectorial quantities meaning that they have directional components. For a single element, the displacement within it is generally approximated as:

$$\boldsymbol{u} \approx \hat{\boldsymbol{u}} = \sum_k \boldsymbol{N}_a \boldsymbol{a}_k^e = \begin{bmatrix} \boldsymbol{N}_i & \boldsymbol{N}_j & \cdots \end{bmatrix} \begin{Bmatrix} \boldsymbol{a}_j \\ \boldsymbol{a}_j \\ \vdots \end{Bmatrix} = \boldsymbol{N}\boldsymbol{a}^e \tag{3.18}$$

where $\mathbf{a}_e$ are the nodal displacements of the element. $\mathbf{N}$ contains so called shape functions who are specific for the element type and make it possible to, by numerical interpolation, calculate the displacement in a point within the element by inserting the coordinates of the point. The shape functions can be expressed in normalized coordinates for which the element is symmetric although it in global coordinates is not. A two dimensional element with four nodes, for instance, is depicted as a square in normalized coordinates as shown in Figure 3.2 together with its shape functions.

Equations (3.19), (3.20) and (3.21) express nodal force, element stress and strain respectively in terms of nodal displacement.

$$\boldsymbol{q}^e = \boldsymbol{K}^e \boldsymbol{a}^e \tag{3.19}$$

$$\boldsymbol{\sigma}^e = \boldsymbol{Q}^e \boldsymbol{a}^e \tag{3.20}$$

$$\boldsymbol{\epsilon} = \boldsymbol{B}\boldsymbol{a} \tag{3.21}$$

where $\boldsymbol{q}$ is the matrix where the forces acting on the nodes are listed, $\boldsymbol{K}$ is the element stiffness matrix and $\boldsymbol{a}$ is, as seen before, the nodal displacements. Similarly the stresses, (3.20), at any point in the element depend on $\boldsymbol{Q}$ which is the element stress matrix. As for strains, (3.21), the matrix $\boldsymbol{B}$ is defined as:

$$\boldsymbol{B} = \boldsymbol{S}\boldsymbol{N} \tag{3.22}$$

where $\boldsymbol{S}$ is a partial differential operator relating strain to displacement for which it is the derivative with respect to space. $\boldsymbol{B}$ is also used for defining $\boldsymbol{K}^e$ an $\boldsymbol{Q}^e$:

$$\boldsymbol{K}^e = \int_{V_e} \boldsymbol{B}^T \boldsymbol{D}\boldsymbol{B} dV \tag{3.23}$$

$$\boldsymbol{Q}^e = \boldsymbol{D}\boldsymbol{B} \tag{3.24}$$

where $\mathbf{D}$ contains the elastics properties of the material. For an isotropic material in a two dimensional space

$$\boldsymbol{D} = \frac{E}{1-\nu^2}\begin{bmatrix} 1 & \nu & 0 \\ \nu & 1 & 0 \\ 0 & 0 & \frac{1-\nu}{2} \end{bmatrix} \tag{3.25}$$

3.6.2. Virtual work formulation

Using the principle of virtual work, an equation can be formulated saying that the external work on the element, (**??**), i.e. the sum of the products of nodal forces and corresponding displacements, must be equal to the internal work, (3.6.1)(3.27). The internal work is that done by stresses and distributed body forces within the element. The virtual work principle introduces a variational factor which represents an arbitrary (virtual) nodal displacement, δa. Also virtual factors for strain, δ, and virtual displacement, δu, are introduced.

$$\delta \boldsymbol{a}^t \boldsymbol{q}^e \tag{3.26}$$

$$v_s = \frac{G}{\rho} \tag{3.27}$$

Now a virtual work equation can be formulated in order to fulfill the equilibrium condition for the element. Using formulation for stress and strain in terms of nodal displacement and some linear algebra, it can be expressed as:

$$\delta \boldsymbol{a}^{eT} \boldsymbol{q}^e = \delta \boldsymbol{a}^{eT} \left(\int_{V_e} \boldsymbol{B}^T \boldsymbol{\delta} dV + \int_{V_e} \boldsymbol{N}^T \boldsymbol{b} dV \right) \tag{3.28}$$

for which the factor δaeT , i.e. the variation of nodal displacement, can be eliminated. Development of (3.28) results in the following equation:

$$\boldsymbol{q}_e = \boldsymbol{K}_e \boldsymbol{a}_e + \boldsymbol{f}_e \tag{3.29}$$

3.6.3. Assembly to global matrix equation

As mentioned above, it is convenient to use normalized coordinates in order to express the physical relations for an element. This requires a transformation of element properties to the global coordinate system so that all element equations can be assembled in one equation system. As physical relations are expressed in terms of nodal displacement, so is the transformation. Thus, in order to fulfill the condition that internal and external work has to be equal in normalized and global coordinates, the relation in (3.30) is used.

$$\boldsymbol{a}' = \boldsymbol{L}\boldsymbol{a} \tag{3.30}$$

where a is the nodal displacements in normalized coordinates and L is a transformation matrix. L is further used to transform the element stiffness matrix in local coordinates, K, to global coordinates.

$$\boldsymbol{K} = \boldsymbol{L}^T \boldsymbol{K}' \boldsymbol{L}' \tag{3.31}$$

Following the transformation is the assembly of all element equations to the global matrix equation on the form:

$$\boldsymbol{K}\boldsymbol{a} = \boldsymbol{r} - \boldsymbol{f} \tag{3.32}$$

where r lists all nodal forces, one for each degree of freedom, with contributions from each element. Recalling Equation (3.29) ,

$$\boldsymbol{r} = \sum_{i=1}^{m} \boldsymbol{q} \tag{3.33}$$

Before solving Equation (3.32), boundary conditions need to be applied. In the case of a static problem this could be for example a prescribed displacement or external force. By replacing unknown quantities with boundary conditions on the to nodes to which they apply, the number of equations is reduced and thus the equation system is solvable.

3.6.4. Dynamic analysis

The main difference in a dynamic analysis of an entity is that the studied quantity, which previously is assumed to be displacement, is a function of time.

$$\boldsymbol{a} = \boldsymbol{a}(t) \tag{3.34}$$

Due to the movement, there will also be inertia and damping forces that need to be accounted for in the equilibrium equation. This is done by introducing the mass matrix, M, and the damping matrix, C, with which acceleration and velocity, i.e., derivatives of a, are multiplied. These matrices are obtained in a manner similar to the stiffness matrix, K. Introducing these two forces results in the following matrix differential equation:

$$\boldsymbol{M}\ddot{\boldsymbol{a}} + \boldsymbol{K}\dot{\boldsymbol{a}} + \boldsymbol{K}\boldsymbol{a} + \boldsymbol{f} = 0 \tag{3.35}$$

4. Implementation

Studying the effect of resonance at the fundamental frequency in soils with respect to train vibrations, estimates of the fundamental frequency at sites previously subject to train vibration measurements are made as well as simulations of transfer functions in Comsol with respect to soil depth. Furthermore, measurements of vibrations from train passages are performed as well as ambient vibrations.

4.1. Phase I - Site effect estimation from geotechnical data

Before performing measurements, sites that are subject to this thesis or sites mentioned in the TVANE report [17] are investigated in terms of soil type and soil depth in order to get a rough estimate on what the possible fundamental frequency of the site could be. For the sites at which measurements already have been carried out and for which results are reported, this investigation aims to show wether or not estimated fundamental frequencies within a certain range correlates with high vibration levels. As no exact measurement positions are given, the fundamental frequency is calculated from the largest soil depth observed on the map.

4.2. Phase II - Calculation of frequency dependent transfer function with FEM

Using COMSOL Multiphysics, transfer functions from a point 10 m from an excited point at the surface to receivers at 50 m distance from the source is calculated. A linear elastic material is assumed. The model is built as shown in Figure 4.1 with three different soil depths. At the surface in the middle, where the soil depth is 15 m, the excitation point is placed. Receivers are placed at the surface where the soil is 20 m and 10 m deep respectively. Density is set to 1800 kg/m^3 and Young's modulus to $0,77 \cdot 10^9$ MPa so that f_0 is 5 Hz for the deep part and 10 Hz for the shallow part according to (3.13). Poisson's ratio is set to $0,49$ assuming completely saturated soil. As boundary conditions, the model has a free surface on top, on the bottom a fixed constraint representing the firm substrate and low reflecting boundaries on the remaining surfaces. On the whole model a gravity load is applied. On the block representing the soil there is a block representing a concrete sleeper onto which periodic load is applied. The frequencies

studied are center frequencies of third octave bands ranging from 1 to 20 Hz. The excitation point is a boundary load subject to a vertical periodic force and from it receivers are placed 10 and 40 m. The model consists of tetrahedra with four nodes and thus linear shape functions. The distance between nodes is aimed to be smaller than a sixth of a wavelength. Regarding shear wave speed of the chosen material and 20 Hz which should yield the shortest wave length, the distance should be 2, 67 m at most. Due to too long computation time with that element size, 3 m between the nodes are chosen as the smallest distance.

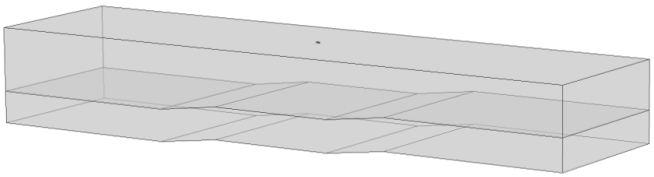

Figure 4.1.: Geometry of Comsol model

4.3. Phase III - Site effect estimation by measuring ambient vibrations

The influence of site effects on amplitudes of ground motion due to train pass bys are analysed by measurements. The measurements are carried out at a meadow next to the railway in Partille. Two measurement sites, further referred to as A and B, are chosen. For each of the sites, accelerometers are placed at 10 m and 50 m distance from the rail. The points close to the rail are further referred to as A1 and B1. Correspondingly, the points far from the rail are called A2 and B2. The soil depth varies along the railway and it is expected that the fundamental frequency is the main factor influencing the response as other factors such as train type, rail condition and soil type are assumed to be constant.

4.3.1. Measurement

One 3-component accelerometer is placed close the rail as a reference point representing the source strength. One far-field 3-component station is placed approximately 50 m from the rail. The measurement station measures during at least half an hour capturing

both ambient seismic vibration as well as train passages. When a train passes, the time from the beginning of the measurement is recorded in order to find it in the signal. In order to record the train speed of the passage, the time it takes for the train to pass two points at a certain distance from each other is measured and then divided by the distance. The sampling frequency is 4kHz.

4.3.2. Data processing

H/V ratio

Data from the ambient measurement is processed in a software provided by Geopsy which is an organisation within the SESAME European Project. The time signals from each station is cut using an anti-trigger algorithm separating stationary parts of the signal from impacts making sure that only ambience is analyzed. The anti-trigger algorithm is based on a short-term average, STA, which is a time average of a short part of a time window and a long-term average, LTA, which is the average level of a complete time window. For a time window to be subject for evaluation $0,8 < STA/LTA < 1,3$ must be fulfilled. The time window for which LTA and STA is evaluated is always 30 seconds and 1 second long respectively. The length of the time windows which are used in the actual H/V-ratio evaluation are chosen with respect to expected fundamental frequency, $f_{0,exp}$. The SESAME User Guidelines suggests that at least ten periods of the lowest frequency of interest should fit into the time window. In this study, $0,5f_{0,exp}$ is chosen as the lowest frequency of interest. For the time windows that pass the STA/LTA-criterion an FFT is carried out for all three components followed by an average of the horisontal components and then a ratio between the horisontal and vertical spectrum yielding the H/V-ratio. An average for all time windows is then made and the resulting spectrum is evaluated according to the SESAME User Guidelines [2] in order to see how reliable an eventual peak representing the fundamental frequency, f_0, is.

Train passage

Each train passage is cut out from the time signal in the signal processing software Artemis. The passage starts at the point at which an increase in level starts and ends at the point at which the level is back at that of the ambient vibrations. The signal is divided into one second long windows with an overlap of 50 % and multiplied with a Hanning window. Each window is then transformed to the frequency domain. Both an average spectrum and a peak value spectrum is calculated. Transfer functions from point A1 and B1 to A2 and B2 respectively are calculated as a difference between third-octave band spectra. Also the actual levels in point A and B are compared in order to see local amplification at the reference point. A part of the signal where no passage

occurs is cut out and evaluated in the same way as the train passages in order compare the level of the passages with the background level. Passages whose level do not exceed the background level are not evaluated.

5. Results

5.1. Investigation of geotechnical conditions

In the report from TVANE, four sites were subject to measurements. For two of them, Falköping and Töreboda, the vibration levels are known to be low which is why only a few samples were recorded to confirm this. The soil depth maps, figures 5.1 and 5.1, acquired from SGU shows that both of the sites has a soil layer which is not more than 10 m deep. The soil type in Falköping around the measurement site is clayey moraine which gives a shear wave speed between 600 and 1000 m/s. The estimated of the fundamental frequency of the sites is according to (**??**) between 15 and 27 Hz. This is a lot higher than the dominating frequency of a train passage. For the remaining two however, the estimated fundamental frequency is around 3 Hz which is much more in the same area as the frequency content of the train passage. All the data is presented in table5.1

Table 5.1.: My caption

	Soil type	E $(\cdot 10^9)$	$\rho(\cdot 10^3)$	ν	d	f_0
Falköping	Clayey moraine	$2.3 - 6.5$	$2.2 - 2.4$	$0,3$	10	15-25
Töreboda	Lera-Silt	$2.3 - 6.5$	$2.2 - 2.4$	$0,3$	10	15-25
Kungsbacka	Postglacial finlera	$2.3 - 6.5$	$2.2 - 2.4$	$0,3$	50	3-5
Alingsås	Postglacial sand	$0.27 - 0.72$	$1.7 - 2.2$	$0,34 - 0,43$	50	1-2

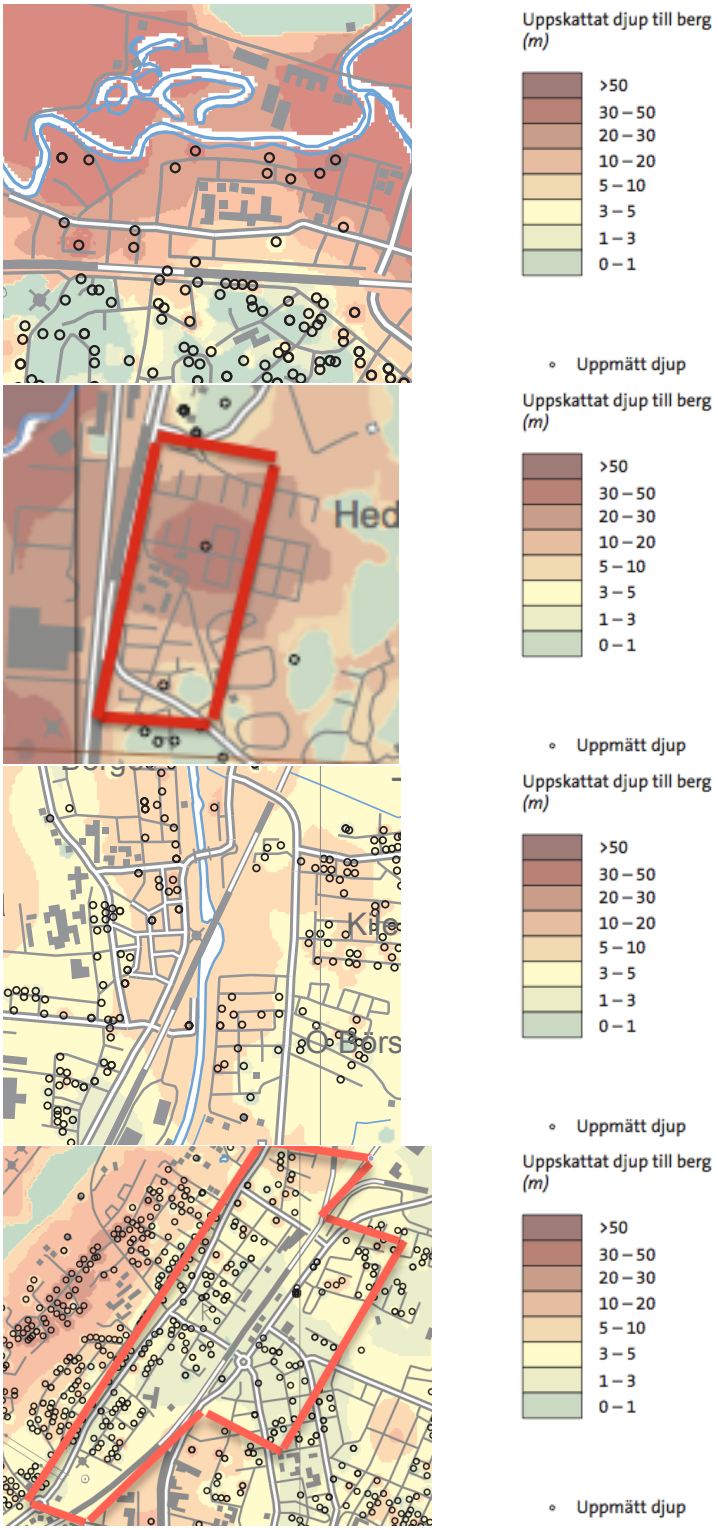

Figure 5.1.: Soil depth maps of (from above) Alingsås, Kungsbacka, Töreboda, Falköping.

5.2. Calculation of transfer functions in FEM

The expected resonance frequencies, calculated from chosen material parameters are, for 10 m, 10 Hz and for 20 m, 5Hz. Plots of frequency responses from the Comsol simulations are shown in Figure 5.2 and transfer functions in Figure 5.3. For both the x-component, which is paralell to the transmission path, and the z-component, which i the vertical, a peak can be observed at $1,6$ Hz for 20 m soil depth and $3.15 - 5$ Hz for 10 m soil depth. This concerns both receiver positions, although the peak is much clearer for 20 m soil depth. Below the respective frequencies the response is very weak compared to the rest of the spectrum. It is also noticable that the peaks occur close to or at the expected fundamental frequencies. This is confirmed, observing the transfer functions, and especially that from the source which shows a clear peak at $1,6$ Hz for 20 m soil depth and $3.15 - 4$ Hz for 10 m soil depth.

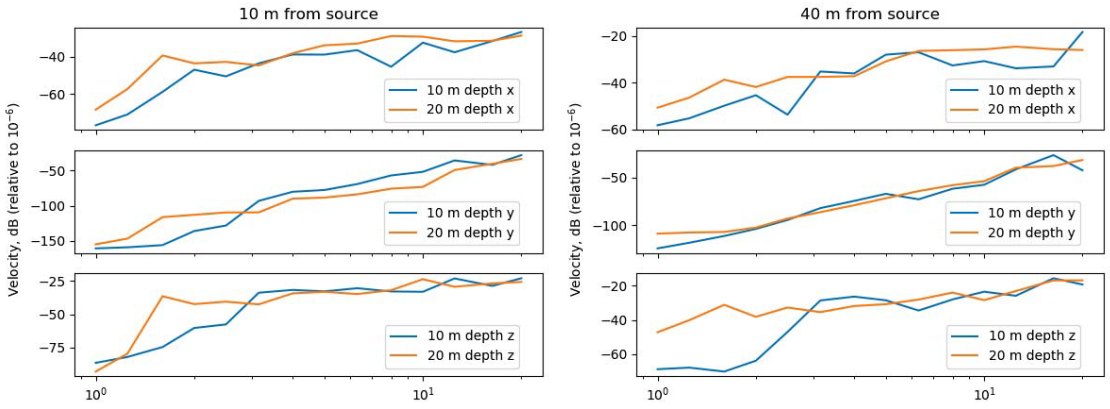

Figure 5.2.: Frequency response at 10 m (left) and 40 m (right) from source. The x-component is shown on the top row, y-component on the middle and z-component on the lowest row.

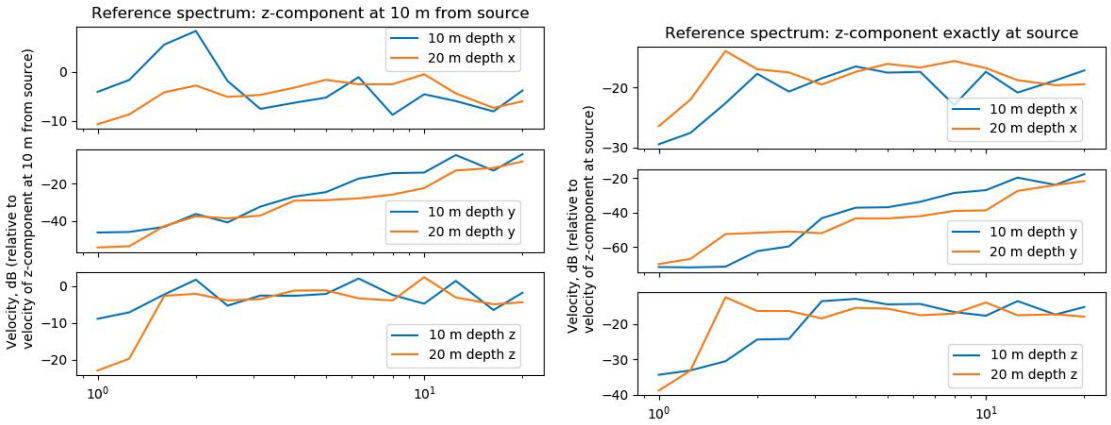

Figure 5.3.: Transfer function to x- (top row), y- (middle row) and z-component (lowest row) respectively at 40 m from source. Reference spectrum from z-component at; 10 m from source (left) and source (right).

5.3. Measurement in Lexby

The measurements were carried out in a meadow in Partille, situated along Västra Stambanan. According to the soil depth map, the soil depth is different at the western and eastern parts of the meadow making it suitable for comparing the response of train passages at soils with, presumably, different fundamental frequencies. Ambient vibrations as well as train passages were measured at three points, of which two successfully, along the rail. The accelerometer was attached to a home made construction shown in figure 5.4 which in turn was beaten down in a hole in the ground and dug down in order to dampen air borne noise as well as attaching to the actual clay in the ground instead of the looser top layer. At each point, the measurements lasted approximately one hour in order to get enough train passages to compare and because the ambient vibration analysis requires a time signal with many stationary windows.

Figure 5.4.: Mounting of accelerometer

Figure 5.5.: Map over Partille with the measurement site marked with red.

Figure 5.6.: Soil depth map over measurement site with measurement points A1, A2, B1 and B2 marked with red.

5.3.1. H/V ratio

By observing the soil depth map the soil depth at the different positions in figure5.6 are estimated as written in table 5.2. Accordingly, in table 5.2 the fundamental frequency f_0 is estimated assuming a shear wave speed for a typical post glacial clay of 600-1066 m/s.

Table 5.2.: Estimated soil depth from soil depth map

A1	30 - 33 m	4,5 - 9 Hz
A2	28 - 30 m	
B1	20 m	7,5 - 13 Hz
B2	17 - 20 m	7,5 - 15 Hz

Results from the measurements of ambient vibrations are shown in Figures 5.7, 5.8, 5.9 and 5.10 respectively. The results are not reliable according to the Sesame User Guidelines which primarily demands an amplification factor $A_0 > 2$. The frequency response of an ambient window also resemble the curve of electrical noise from the transducer. However, the frequencies identified as f_0 do agree with what could be expected considering the soil depth in that sense that lower f_0 is found on the spots with deep soil and vice versa.

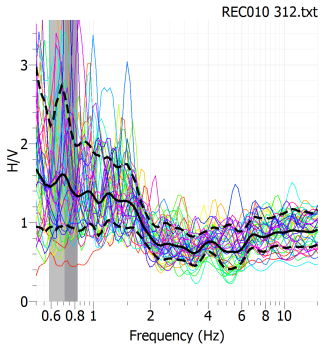

Figure 5.7.: Position A1

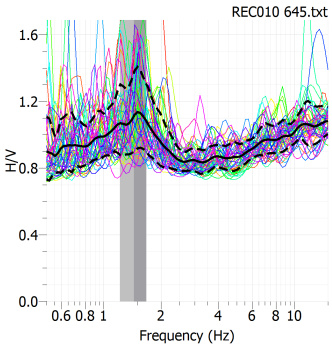

Figure 5.8.: Position A2

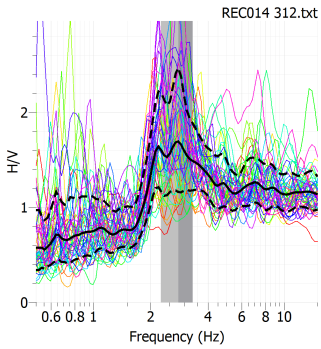

Figure 5.9.: Position B1

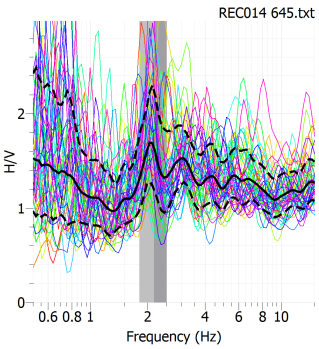

Figure 5.10.: Position B2

5.3.2. Train passages

In this subsection, A1 and B1 are referred to as reference points. A2 and B2 are referred to as field points. In order to compare site A and B, frequency responses for measurements of train passages at both sites are shown in the same graph for reference point, field point and the difference between them respectively. All passages are sorted by train type. In this section, the passages of Regina trains are shown whereas passages from other train types are shown in Appenix A. The signals containing the passages are processed with two different approaches. As a number of time windows fit into the duration of the train passage it is either an average or a peak value of the levels of all time windows for each frequency. Observing the graphs a few trends can be observed. Firstly, for all train types there is less difference between field and reference for site A than site B below at least 6 Hz. Some passages even show a stronger response at the field point. Another trend that is valid for all train types is that the response is stronger at B1 than A1 for frequencies below 5 Hz. For the field response no clear trend can be seen other than that the difference between A2 and B2 is small.

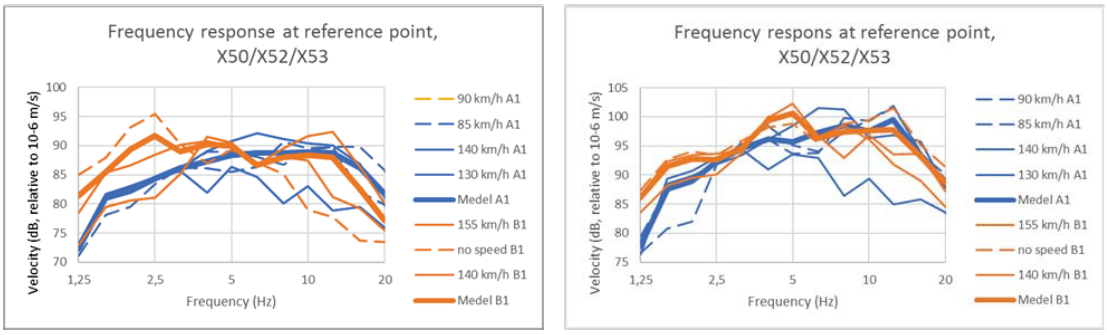

Figure 5.11.: Reference point, left: average, right: peak hold.

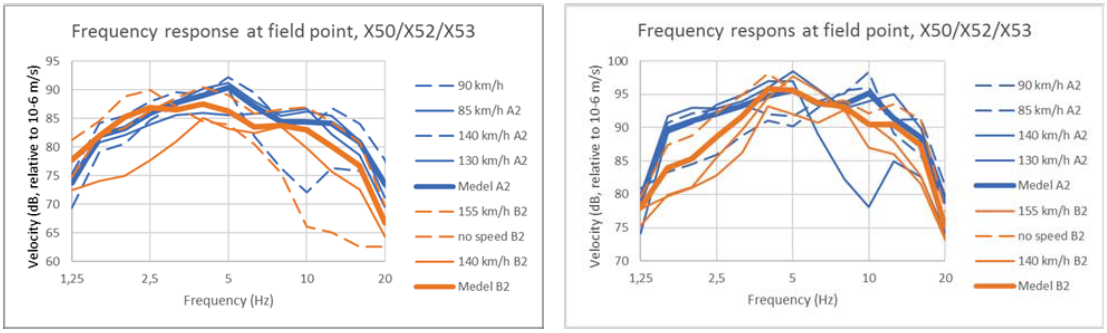

Figure 5.12.: Field point, left: average, right: peak hold.

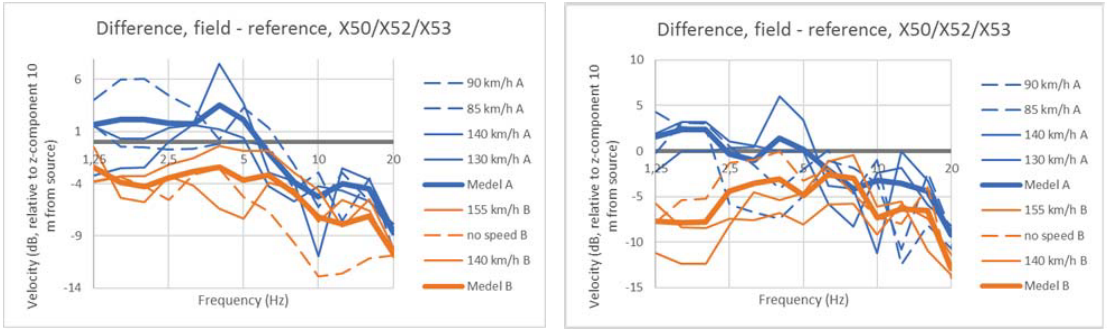

Figure 5.13.: Difference between field and reference, left: average, right: peak hold.

6. Discussion

The literature study and estimation of fundamental frequencies for measurement sites in TVANE indicates that the fundamental frequency, f_0, does have some influence on the wave propagation in that sense that very little wave energy below f_0 is transmitted from the wave source. Due to limited data on exact location of the measurement and roughly estimated geotechnical properties, however, no conclusions about amplification can be drawn.

The FEM-calculations agree with the statement that little energy is transmitted below the expected resonance frequency. The frequency in the FEM-calculations, however, do not agree with the expected frequency. Instead it is two or three third octave bands lower than the expected frequency. As for an eventual amplification at the resonance frequency, peaks are observed in the frequency responses that could confirm a minor amplification. This peak is somewhat clearer in the frequency response close to the source. The transfer function from the source to the point 40 m away also shows a peak at this frequency which could be regarded as an amplification. In this regard, this transfer function is a good complement to those obtained by measurements as it was not possible to measure at the very source. The transfer function from a reference source 10 m from the source has a peak at a frequency which is lower than the peak in the transfer function with referense at the actual source. This is interesting as the peak likely depends on the low level at the reference source rather than a large amplification. Thus, an indication that the reference could suffer from near field effects arises.

Central for this study however, are the measurements of train passages and ambient vibrations. Although the results from the H/V-ratio from the ambient vibration measurements do not fulfill the requirements for reliability specified in the Sesame User Guidelines, the fundamental frequencies obtained are not unexpected as the lowest and second lowest f_0 is found at the largest and second largest estimated soil depth respectively. As measurements were carried out at only four points, though, there is too little data to speak of any correlation. What also might support the results from the H/V-ratios is the apparent amplification of train passages at point A2 occuring around $1,6$ Hz which is the same frequency obtained from the H/V-ratio. Considering the lower f_0 at A1 there could be a concentration of wave energy due to decreasing soil depth as well as amplification. Comparing this to point B1 and B2, f_0 goes from higher

to lower along the propagation path which could indicate that the wave energy that could be amplified at f_0 in point B2 is not transmitted from point B1, hence no amplification on that frequency. However, it must be considered that the responses at the field points for the two site do not differ that much. That implies that an amplification at the field point or a blocking of wave energy at the reference point is not really what happens but rather resonant phenomena close to the rail.

An important observation that finds support in both the measurements and the FEM-calculations is that the response close to the rail or point source, respectively, seem to be affected by the proximity to the source. Also supporting this behaviour is the theory of attenuation properties of body waves and surface waves, described in section **??**, saying that body waves, i.e. shear waves and pressure waves, attenuates faster than surface waves. As f_0 is the frequency at which shear waves are amplified, the influence of shear waves, and by extension f_0, have a minor impact on the far field response, whereas the zone close to the rail could be affected. It should be mentioned, however, that the attenuation properties are derived with respect to an homogenous, isotropic, linear elastic half space which neither the FEM-model nor the measurement site is.

7. Conclusion

The aim of this thesis was to study amplification of train vibrations with a hypothesis that a measurement method, the H/V-method, used in seismology for predicting strong motions of earthquakes could also be applied to trains as vibration source. The method seeks to find a resonance frequency of the soil, f_0, which depends on the thickness of the top layer, i.e, the distance from the soil surface to the bedrock or to an interface to a soil layer with much higher impedance, as well as on the stiffness of the top layer.

The hypothesis was mainly studied by doing measurements of train vibrations and of ambient vibrations which is the scope of the H/V-method. At two sites, close to each other but with different soil depth, measurements were carried out at 10 m from the rail and 40 m from the rail simultaneously in order to obtain a transfer function. Additionally, a previous study concerning train vibrations was reviewed seeking coherence between strong motion and soil depth. Finite element calculations was also performed in order study general behaviour of soil vibrations with respect to soil depth.

The review concluded, that a large soil depth where the measurements were carried out, coincided with large measured amplitudes. The finite element calculations showed an indication of a resonance but not at the expected f_0, calculated with respect to soil depth and shear wave velocity of the soil. Furthermore, the FEM-calculations showed that transfer functions with reference point exactly at the source position and 10 m from it gave incoherent results, indicating that the frequency response close to the source position could be more affected by resonance phenomena than far from the source due to the occurence of body waves. The measurements of ambient vibrations suffered from insufficient sensitivities of the sensors, resulting in unreliable results for f0. The measurements of vibrations from train passages were more succesful and it could be concluded that the difference between measurement positions at 40 m from the rail was little despite different soil depth. For the measurement positions closer to the rail, however, the measured amplitudes at the position with shallower soil clearly dominated over that with deep soil in the frequency range $1 - 5$ Hz.

Finally, there is no indication, supported by both FEM-calculation and measurements, that an amplification occurs in the far field due to f_0. There is an indication that the response close to the source is affected by f_0 and that considering a position

close to, but not exactly at, the source position as reference source could be problematic when estimating decay functions for a site. There is however too little measurement data to make any firm conclusions.

Bibliography

[1] *Framtidsplan för järnvägen: Effektbeskrivning av föreslagna åtgärder 2014-2015*. Banverket, 2003.

[2] *Guidelines for the Implementation of the H/V Spectral Ratio Technique on Ambient Vibrations*. European Commission – Research General Directorate, 2004.

[3] L Auersch. Wave Propagation in Layered Soils: Theoretical Solution in Wavenumber Domain and Experimental Results of Hammer and Railway Traffic Excitation. *Journal of Sound and Vibration*, 1994.

[4] L. Auersch and S. Said. Attenuation of ground vibrations due to different technical sources. *Earthquake Engineering and Engineering Vibration,*, 1994.

[5] COWI. Ny Vibrationsmodel. Technical report, Bane Danmark, 2015.

[6] O Fröidh. *Resande och trafik med Gröna tåget*. KTH Royal Institute of Technology, 2010.

[7] C. E. Hanson, J. C. Ross, and D. A. Towers. High-speed ground transportation noise and vibration impact assessment. Technical report, Federal Railroad Adminstration, 2012.

[8] H.V.C. Howarth and M.J. Griffin. The relative importance of noise and vibration from railways. *Applied Ergonomics*, 21(2):129 – 134, 1990.

[9] R. Klaeboe, I.H. Tununen-Rise, L. Haawrik, and C. Madshus. Vibration in dwellings from road and rail traffic - part ii: exposure-effect relationships based on ordinal logit and logistic regression models. *Applied Acoustics*, 2003.

[10] V. Knall. Railway noise and vibration: Effects and criteria 193(1):9 – 20. *Journal of Sound and Vibration*, 1996.

[11] G. Kouroussis, D. P. Connolly, and O. Verlinden. Railway-induced ground vibrations - a review of vehicle effects. *International Journal of Rail Transportation*, 2014.

[12] V.V. Krylov. *Noise and Vibration from High-Speed Trains*. ICE Publishing, 2001.

[13] H. Lamb. On the propagation of tremors over the surface of an elastic solid. Technical report, University of Manchester, 1904.

[14] Bahrekazemi M. *Train Induced Vibrations and Its Prediction*. PhD thesis, Royal Institute of Technology, 2004.

[15] G. Malm, N. Andersson, and S. Sundgren. Höghastighetsbanor - ett samhällsbygge för stärkt utveckling och konkurrenskraft (SOU 2009:74). *Statens offentliga utredningar*, 2009.

[16] T.M. Meloni. *Wahrnehmung und Empfindung von komplexen, kombinierten Belastungen durch Vibration und Schall*. PhD thesis, ETH Zürich, 1991.

[17] Jerson P Ögren J. Mätning och beräkning av buller och vibrationer från tågtrafik inom TVANE-projektet. Technical report, VTI, 2011.

[18] E. Öhrström, G. Gunnarsson, M. Ögren, and T. Jerson. Slutrapport Forskningsprojektet TVANE. Technical report, Sahlgrenska Akademien vid Göteborgs Universitet, 2011.

[19] Shamsher Prakash. *Soil Dynamics*. McGraw-Hill, Inc., 1981.

[20] Massarch K. Rainer, Bodare Anders, and Smekal Alexander. Effects of Vibrations from Train Traffic. Technical Report 1, Banverket, 2002.

[21] Milutin Srbulov. *Ground Vibration Engineering*. Springer Science + Business Media, 2010.

[22] H. G. Wessberg and C. Håkansson Boman. Infrastruktur och bostäder - ett gemensamt samhällsbygge (SOU 2017:107). Technical report, Statens offentliga utredningar, 2017.

[23] Nakamura Y. A Method for Dynamic Characteristics Estimation of Subsurface Microtremor on the Ground Surface. Technical report, Railway Technical Research Institute, 1989.

[24] Nakamura Y. On the H/V Spectrum. In *The 14th World Conference on Earthquake Engineering*, 2008.

[25] J.A. Zapfe, H.J. Saurenmann, and S. Fidell. Human response to ground-borne noise and vibration in buildings caused by rail transit: Summary of the tcrp d-12 study. In *Notes on Numerical Fluid Mechanics and Multidisciplinary Design*, 2012.

[26] W. Zhang and K. Matsunami. A comparison of site-amplification estimated from different methods using a strong motion observation array in Tangshan, China. In *12th World Conference on Earth Quakes*, 2000.

A. Measurement results

A.1. X2

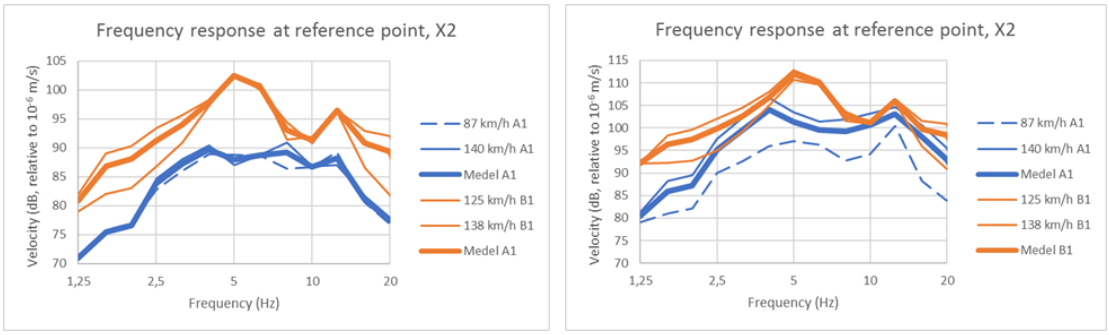

Figure A.1.: Reference point, left: average, right: peak hold.

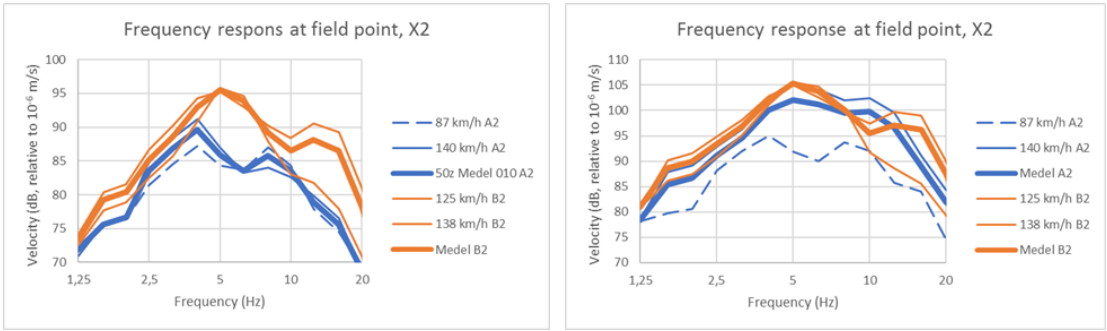

Figure A.2.: Field point, left: average, right: peak hold.

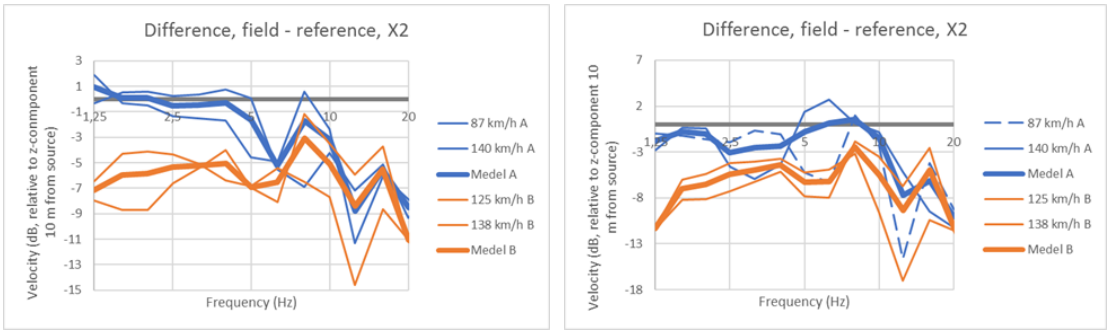

Figure A.3.: Difference between field and reference, left: average, right: peak hold.

A.2. Freight train

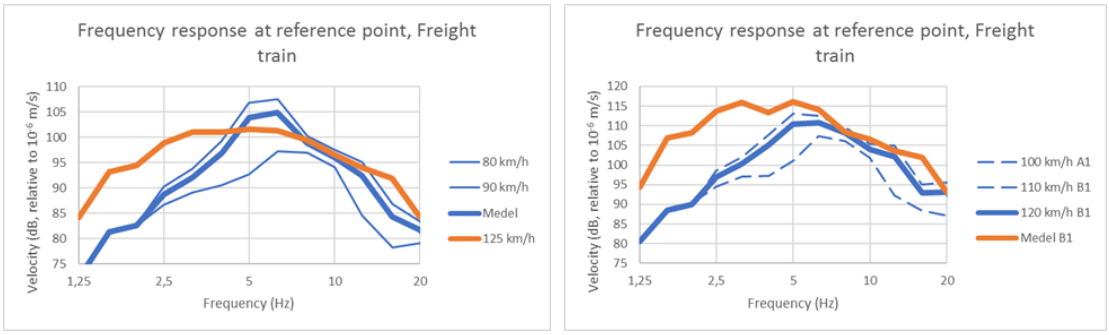

Figure A.4.: Reference point, left: average, right: peak hold.

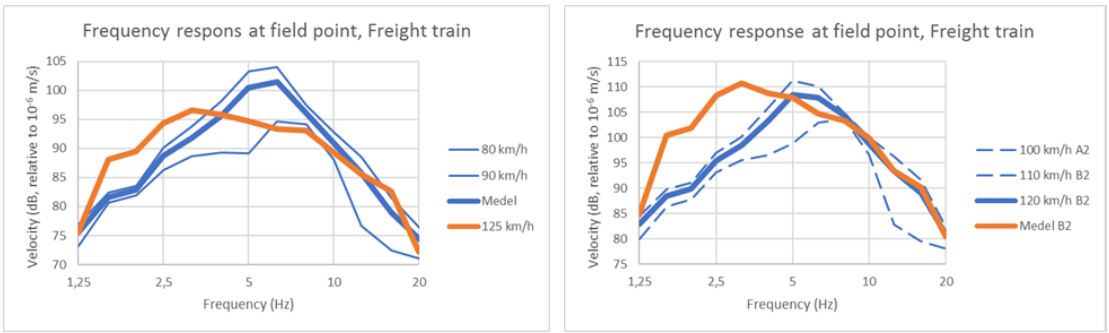

Figure A.5.: Field point, left: average, right: peak hold.

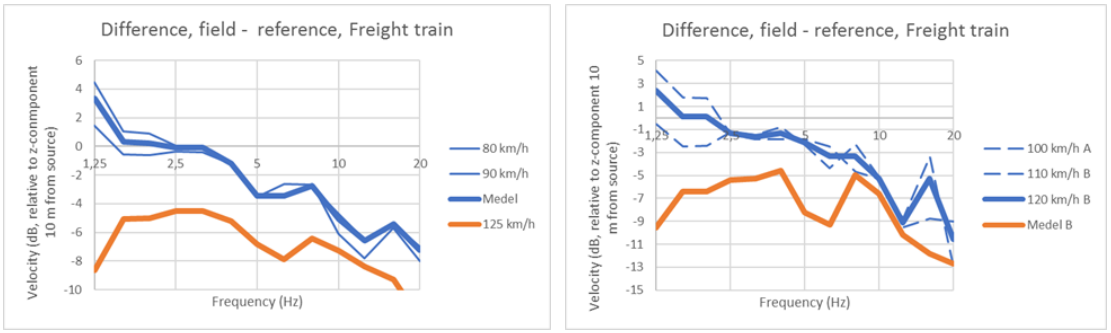

Figure A.6.: Difference between field and reference, left: average, right: peak hold.